MATERIALE PLASTICE
https://revmaterialeplastice.ro
https://doi.org/10.37358/Mat.Plast.1964

Antitumor Effect and Pharmacological Mechanism of Paclitaxel-loaded Silk Fibroin Nanomaterials on H22 Subcutaneous Tumor Model of Mouse Hepatoma

SHENGXING ZHAO*
Department of pharmacy, Anhui University of Chinese Medicine, Hefei City 230012, China

Abstract:*This work was developed to analyze the adoption of paclitaxel-loaded silk fibroin nanoparticles (SFNPs) in subcutaneous transplanted tumor model of mouse hepatoma to explore its anti-tumor effect. Twenty-five specific pathogen-free (SPF) mice were selected to construct a subcutaneous tumor model of liver cancer, and they were randomly rolled into control group, group A, group B, group C, and group D, with five mice in each group. The silk fibroin was mixed with an organic solvent to prepare a suspension, and the SFNPs were prepared through centrifugation, ultrasound, and other methods. The paclitaxel-loaded SFNPs were prepared by mixing paclitaxel and silk fibroin aqueous solution, centrifuging, washing, and dispersing. Then, the five groups of mice were intervened by different dosage regimens to analyze the changes of various indicators. As a result, the prepared nanoparticles had uniform particle size, uniform distribution, no adhesion, and the average particle size was less than 500 nm. The tumor volume of mice in groups C and D on the 7th, 9th, and 13th days of administration were dramatically smaller than those in the control group, group A, and group B ($P < 0.05$). And the tumor volume (154.49 ± 9.65 mm^3) of mice in group D on the 13th day of administration was dramatically smaller than that in group C (167.79 ± 9.72 mm^3) ($P < 0.05$). The tumor mass (0.89 ± 0.14 g, 0.54 ± 0.13 g, and 0.46 ± 0.11 g) of mice in groups B, C, and D was dramatically smaller than that in the control group and group A (1.23 ± 0.12 g, 1.24 ± 0.11 g) ($P < 0.05$), and that of group D was dramatically smaller than groups B and C ($P < 0.05$). The apoptosis rates of tumor cells in groups C and D (46.38%, 48.23%) were greatly superior to those in the control group (16.7%), group A (21.33%), and group B (35.6%) ($P < 0.05$), and that of group D was greatly superior to that in group C ($P < 0.05$). In summary, paclitaxel-loaded SFNPs can effectively improve the targeting effect and bioavailability of drugs in the treatment of liver cancer, thereby improving the efficacy, and had a good application prospect.*

Keywords: *silk fibroin, nano-drug delivery system, liver cancer, paclitaxel, targeting, apoptosis*

1. Introduction

Malignant tumors can invade and compress surrounding tissues and organs, and are easy to metastasize and relapse, causing serious harm to human life and health and being a major public health problem facing the world at present [1]. Liver cancer is a malignant tumor occurring in the liver, the largest organ of the human body. It is generally classified into primary liver cancer and secondary liver cancer according to its etiology and other factors [2,3]. Primary liver cancer includes hepatocellular carcinoma, intrahepatic cholangiocarcinoma, cholangiocarcinoma, angiosarcoma, hemangioendothelioma, and hepatoblastoma [4]. Most hepatocellular carcinoma mainly develops from cirrhosis. Intrahepatic cholangiocarcinoma is the most common liver cancer, accounting for about 15% of liver cancer. There are no obvious symptoms in the early stage of the disease, but with the aggravation of the disease, patients may suffer from weight loss, loss of appetite, nausea and vomiting, abdominal pain, and abdominal distention [5,6]. At present, studies on the etiology of liver cancer have not reached a clear conclusion, and it is generally believed that it is related to gene mutations, most of which are mutations caused by the acquired environment [7,8]. In addition, it may be associated with hepatitis virus infection, cirrhosis, and other factors. The treatment of liver cancer includes local treatment (surgical treatment, ablation, embolization, and radiotherapy) and systematic treatment (targeted drug

*email: m18356013033@163.com

therapy, immunotherapy, etc.). Corresponding treatment measures should be formulated according to patients' symptoms, disease stages, and types [9,10]. Targeted drugs can be used to treat cancer-causing mutations, and targeted drugs are the first choice for patients with advanced liver cancer [11].

Paclitaxel is an anti-microtubule anti-tumor drug that has anti-tumor effects on some malignant melanoma, leukemia, and malignant sarcoma cell lines [12,13]. The drug binds to microtubules and prevents them from separating chromosomes when cells divide, leading to cell division, especially death of rapidly proliferating cancer cells [14,15]. However, paclitaxel used in the treatment of tumor often has certain side effects on patients. The patients are firstly manifested as nausea and vomiting caused by gastrointestinal mucosal damage, loss of appetite, etc. In addition, patients are prone to nerve endings damage and allergic reactions [16,17]. With the development of nanotechnology and the synthesis and application of polymer materials with good biocompatibility or biodegradation, the research of novel molecularly targeted drugs and their drug carriers in the field of tumor therapy has attracted increasing attention [18,19].

Studies found that polymer carriers have good biocompatibility and targeting advantages, which can play an important role in tumor therapy [20,21]. Therefore, silk fibroin protein was mixed with organic solvent to prepare suspension, and silk fibroin protein nanoparticles were prepared through centrifugation, ultrasound, and other methods. The silk protein nanoparticles loaded with paclitaxel were prepared by centrifugation, washing, and dispersion after mixing of paclitaxel and silk protein solution. Then, the anti-tumor effect of silk fibroin nanomaterial loaded with paclitaxel was studied in mouse liver cancer model, to provide some basis for the treatment of malignant tumors.

2. Materials and methods

2.1. Experimental animals and grouping

Twenty-five healthy adult male specific pathogen-free (SPF) mice were purchased from the animal experimental center, weighing about 28 g and aged 7-8 weeks. According to SPF animal feeding requirements (temperature: 18-29℃, daily temperature difference ≤3℃, relative humidity controlled at about 50%, fresh air ventilation times 10 times/h, airflow speed ≤ 0.18m/s, pressure difference = 25Pa, cleanliness at level 10,000, ammonia concentration 15mg/m^3, feeding environment noise ≤ 60 dB), they were kept in a barrier system. The microbial status in the feeding, management, and experimental operation of SPF animals was strictly controlled.

2.2. Preparation of SFNPs

Silk fibroin (Suzhou Simete Biotechnology Co., LTD.) was dissolved in water and stood for 2-8 h at 2-6℃ to obtain a silk fibroin solution with a concentration of 10-50 mg /mL. The silk fibroin protein solution was mixed with organic solvent ethanol (99.5%, Shanghai Jizhi Biochemical Technology Co., LTD.), methanol (99.5%, Shanghai Jizhi Biochemical Technology Co., LTD.), or acetone (99%, Guangdong Wengjiang Chemical Reagent Co., LTD.) with a volume ratio of 1:4-8, and stirred (the mixing temperature was 20-60^{o}C), so that the nanoparticles suspension was obtained [22,23]. The prepared nanoparticle suspension was centrifuged for 30 min at 8,000-20,000 rpm and 4^{o}C. After centrifugation, the nanoparticles were re-dispersed and washed by deionized water and centrifuged again to obtain precipitation [24,25]. The prepared nanoparticles were precipitated and mixed with water, and the silk fibroin protein nanoparticles were obtained by ultrasonic treatment.

2.3. Preparation of paclitaxel-loaded SFNPs

2 mg paclitaxel (purity >99%, Jiangsu Yew Pharmaceutical Co., LTD.) was dissolved in ethanol solution (Shanghai JiZhi Biochemical Technology Co., LTD.), with silk fibroin aqueous solution added into it drop by drop, and the mixture was constantly stirred to make the solution milky white. The undissolved impurities in the solution system were removed by filtration [26], centrifuged for 30 min at 2-5^{o}C and 15,000-16,000 rpm, and the separated precipitates were re-dispersed. After repeated centrifugal washing, water was added for ultrasonic re-dispersion to obtain silk protein nanoparticles

loaded with paclitaxel [27,28]. Figure 1 showed the high gravity device prepared by silk fibroin protein nanoparticles.

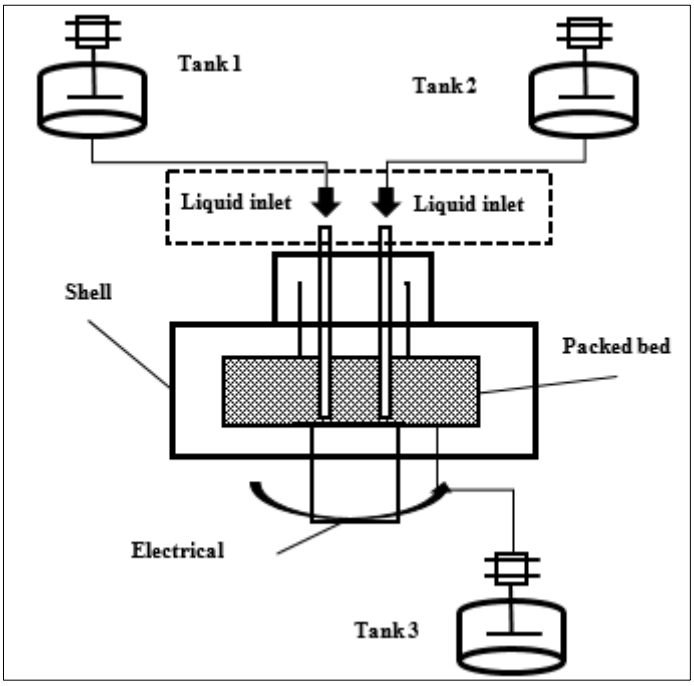

Figure 1. Hyper-gravity device system

2.4. Characterization and analysis of SFNPs

Information on various physical and chemical properties of the tested sample itself, such as morphology and composition information, was obtained through scanning electron microscope (SEM) (Suzhou Fei Shiman Precision Instrument Co., Ltd.).

The particle size of silk fibroin nanoparticles was determined by Brookheaven B1-900AT dynamic light scattering (DLS), and the zeta potential was determined by Brookheaven Plus zeta potential. All measurements were made 3 times at 25°C.

The uptake of silk fibroin nanoparticles was observed by Olympus fluorescence microscope (Shanghai Pucher Optoelectronics Technology Co., Ltd.).

2.5. Construction of mouse liver cancer subcutaneous tumor model

H22 mouse hepatoma cell lines (purchased from Shanghai Tongwei Biotechnology Co., LTD.) were thawed and centrifuged in a sterile environment of ultra-clean workbench, followed by addition of fetal bovine serum and inoculation. 0.2 mL H22 mouse hepatocellular carcinoma cell line was inoculated into the right back subcutaneous tumor of SPF mice to construct mouse hepatocellular carcinoma subcutaneous tumor model. Five days after modeling, tumor growth and partial redness of skin were observed on the back of mice. When the tumor volume of mice reached 100 mm^3, the mice were randomly divided into five groups, including control group and observation group (group A, B, C, and D), with five mice in each group. After grouping, each mouse was labeled according to group.

On the same day after grouping, mice in control group were intraperitoneally injected with normal saline, mice in group A were intraperitoneally injected with 65 mg/Kg silk fibroin, mice in group B were intraperitoneally injected with 10 mg/Kg paclitaxel-loaded SFNPs, mice in group C were intra-peritoneally injected with 10 mg/Kg paclitaxel-loaded SFNPs, and mice in group D were injected with 10 mg/Kg paclitaxel-loaded SFNPs around tumor after anesthesia. After that, mice were given drugs in the above way on day 5, day 9, and day 13, respectively. The mice were sacrificed the next day after the last drug administration. Tumor and viscera of mice in each group were removed for embedding, hematoxylin-eosin staining (HE), and observation and recording.

2.6. Observation indicators

The five groups of mice were given different drugs, and the serum, liver, and kidney function indicators of mice were detected such as Alanine Transaminase (ALT) and Aspartate aminotransferase (AST) content, liver tissue and tumor tissue staining, tumor volume change, and tumor inhibition rate. The tumor tissue was prepared into single cell suspension and Annexin V FITC/PI staining method was used to detect the proportion of apoptosis of tumor cells, where, the tumor volume calculation is shown in equation (1).

$$V\left(mm\right)=0.4mn \tag{1}$$

where, m represents the maximum tumor diameter (mm), n represents the minimum tumor perpendicular to m. The calculation method of tumor inhibition rate is shown in equation (2).

$$Tumor\ inhibition\ rate=\left[1-(\frac{V_1}{V_0})\right]\times 100\% \tag{2}$$

V_0 represents the average tumor volume in the control group, and V_1 represents the average tumor volume of the treatment group.

2.7. Statistical methods

Data processing was analyzed by SPSS 22.0. The measurement data were in the form of mean ± standard deviation ($\overline{x}\pm S$), and the counting data were in the form of percentage (%). Analysis of variance was used for pairwise comparison. $P < 0.05$ indicated that the difference was statistically significant.

3. Results and discussions

3.1. Silk fibroin nanoparticle characterization

Colloidal particles with a particle size in the range of 10 - 1,000 nm formed by encapsulating drugs into carrier materials by chemical cross-linking or electrostatic adsorption are called nanoparticles, and both water-soluble and lipid-soluble drugs can be used in nanoparticle delivery systems [29, 30]. In addition, by linking some specific groups on the surface of nanoparticles, the specific binding effect can be used to improve the uptake of nanoparticles by cells [31,32]. Figure 2 shows the SEM images of SFNPs prepared by mixing silk fibroin with organic solvent and by centrifugation, ultrasound, and other methods. Figure 2C, Figure 2D, Figure 2E, and Figure 2F show that the prepared nanoparticles had uniform particle size, uniform distribution, no adhesion, and average particle size less than 500 nm.

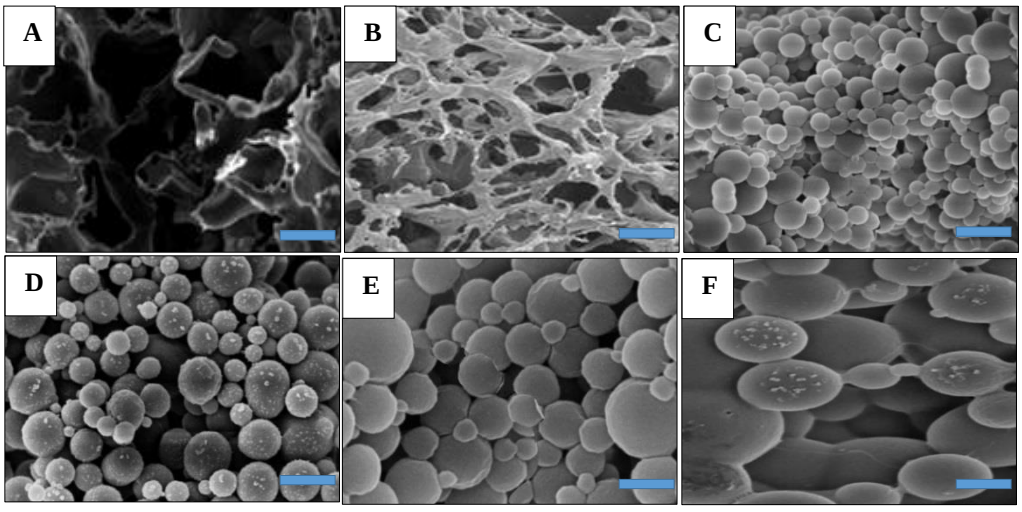

Figure 2. Electron microscope images of nanoparticle characterization.
Note: the scales in Figures A, B, C, D, E, and F indicated
100 μm, 50 μm, 10 μm, 5 μm, 1 μm, and 500 nm, respectively

3.2. Imaging of different solvents on nanoparticle size

To study the changes of particle size, polydispersity, and other properties of SFNPs prepared with different solvents, ethanol, methanol, and acetone were used to prepare silk fibroin nanoparticles, and their particle size and ξ potential were compared. The results were shown in Table 1. The results showed that when the solvent was ethanol and the silk fibroin content was 5 mg/mL, the particle size of the prepared nanoparticles was the smallest and the polydispersity of the nanoparticles was the lowest. When ethanol, methanol, and acetone were used as solvents, the ξ potential of the solution system did not change significantly. Therefore, ethanol was used as solvent in this study to prepare corresponding nanoparticles.

Table 1. Changes of particle size and properties of nanoparticles

Solvent	Silk fibroin/ paclitaxel	Silk fibroin concentration (mg/mL)	Particle size (nm)	Polydispersity	ξ potential (mV)
Ethanol	5:1	2	203.1±2.4	0.161±0.018	-8.23
Ethanol	10:1	5	180.2±2.3	0.13±0.021	-19.83
Ethanol	5:1	5	156.3±1.98	0.108±0.017	-2.53
Ethanol	5:1	10	170.9±2.02	0.142±0.023	-12.14
Methanol	5:1	5	188.7±1.76	0.139±0.02	-2.45
Acetone	5:1	5	213.4±2.43	0.235±0.01	-2.3

3.3. Silk fibroin nanoparticle uptake results

Fluorescein was taken as the drug loaded on SFNPs, and the uptake of H22 mouse liver cancer cells was analyzed. The fluorescence observation results were shown in Figure 3. Fluorescent spots were observed in the cytoplasm and around the nucleus of the cells, but no green fluorescent spots were observed in the nucleus, which indicated that the drug-loaded SFNPs (silk fibroin: paclitaxel =5:1; silk fibroin concentration: 5 mg/mL) were absorbed by H22 mouse hepatoma cells in a short period of time, thus exerting pharmacological effects on them.

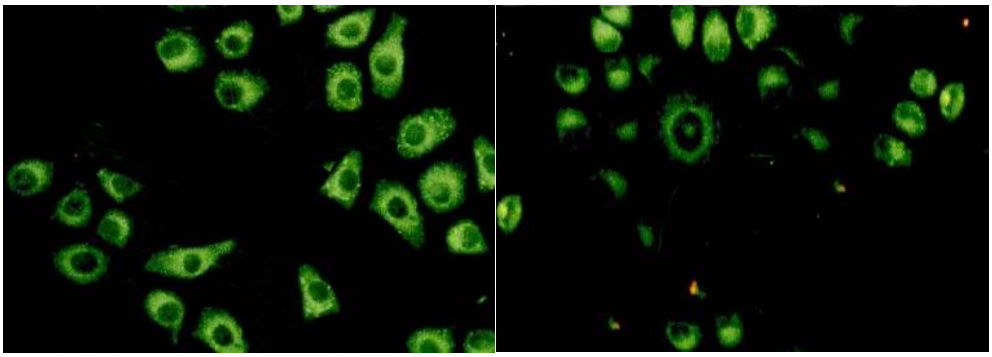

Figure 3. H22 uptake of SFNPs

3.4. Effects of paclitaxel and silk fibroin concentrations on hepatocytes

To analyze the toxic effects of paclitaxel and silk fibroin on hepatocytes, the activity of mouse hepatocytes at different concentrations was compared, and the results were shown in Figure 4. Among the five groups of mice, the dosing regimens of mice in groups B, C, and D included paclitaxel, and the dosing regimens of mice in groups A, C, and D included silk fibroin. Therefore, the cell activity of mice in groups B, C, and D at different concentrations of paclitaxel and that of mice in groups A, C, and D at different silk fibroin concentrations were compared, but no obvious cytotoxicity was found.

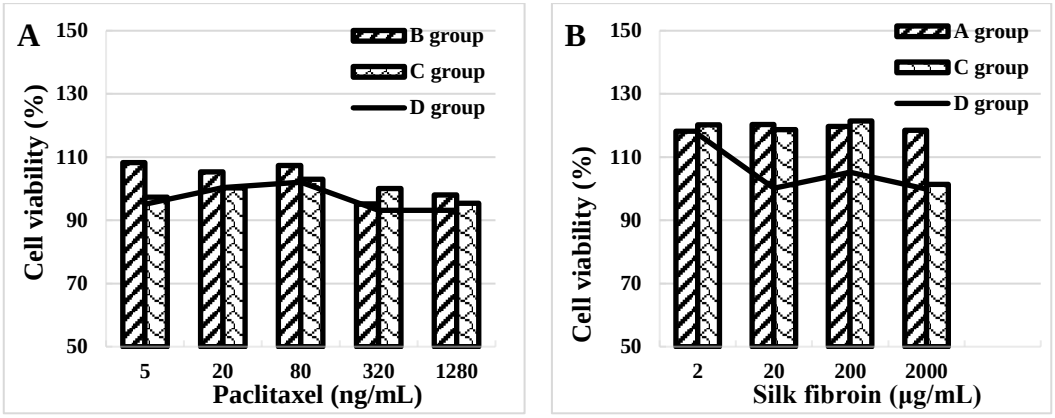

Figure 4. Cytotoxic effects of paclitaxel and silk fibroin at different concentrations.
Note: A represented different paclitaxel concentrations; B represented different silk fibroin concentrations

3.5. Changes in tumor volume and mass in five groups of mice

After the five groups of mice were administered according to different regimens, the tumor volume and mass changes of each group of mice were measured and calculated on the 1st, 3rd, 5th, 7th, 9th, and 13th days of administration. The results were shown in Figure 5. Figure 5A showed the changes in tumor volume of mice in the five groups on different days of administration. With the prolongation of time, the tumor volume of the mice gradually increased, and the tumor volume of the control group, group A, and group B continued to increase, but without substantial difference between them (P>0.05). On the 9th day after administration, the tumor volume of group C and group D no longer increased, and then gradually decreased. The tumor volume of mice in group C and group D on the 7th, 9th, and 13th days of administration were dramatically smaller than those in the control group, group A, and group B (P < 0.05). And the tumor volume of mice in group D (154.49 ± 9.65 mm^3) on the 13th day of administration was dramatically smaller than that in group C (167.79 ± 9.72 mm^3) (P < 0.05).

Figure 5B showed the comparison results of tumor mass in mice in five groups. The tumor mass (0.89 ± 0.14 g, 0.54 ± 0.13 g, and 0.46 ± 0.11 g) of mice in groups B, C, and D was dramatically smaller than that in the control group and group A (1.23 ± 0.12 g and 1.24 ± 0.11 g) (P < 0.05), and that of group D was dramatically smaller than groups B and C (P < 0.05).

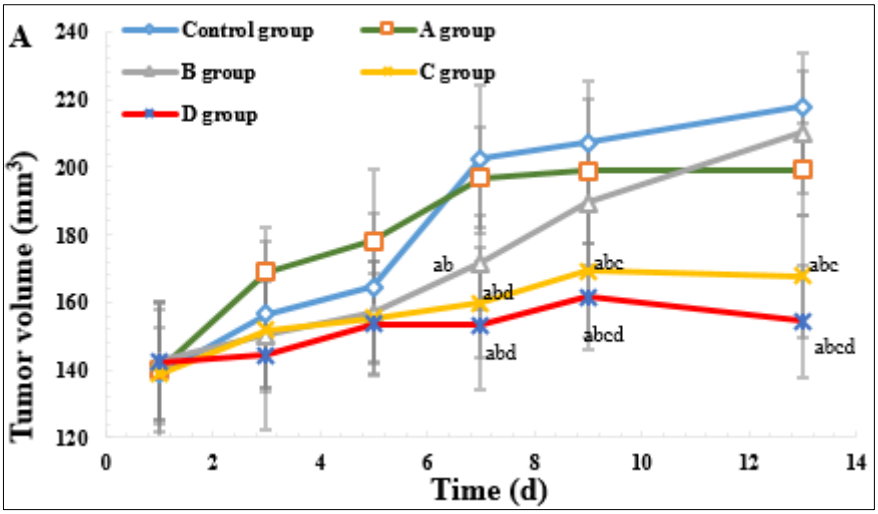

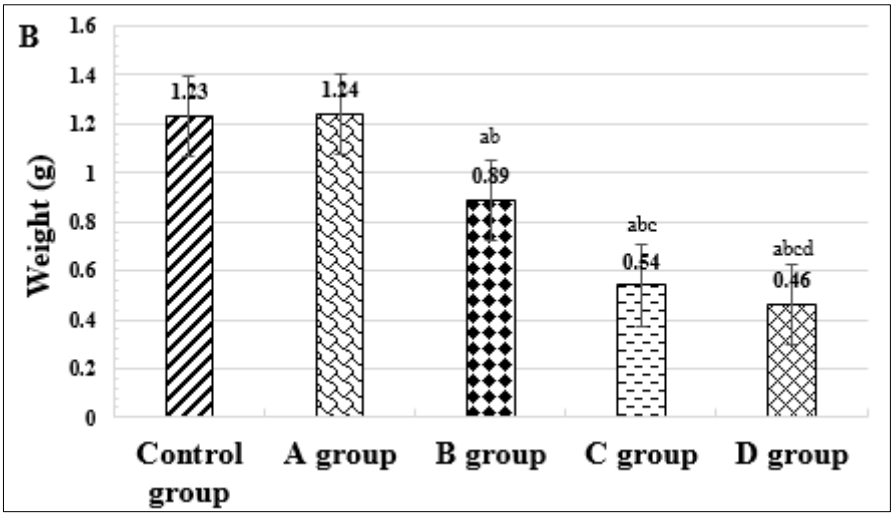

Figure 5. Changes in tumor growth in mice
Note: A: tumor volume; B tumor mass. (Compared with the control group, $^{a}P < 0.05$; compared with the group A, $^{b}P < 0.05$; compared with the group B, $^{c}P < 0.05$; compared with the group C, $^{d}P < 0.05$.)

3.6. Changes of serum indicators in mice

After the five groups of mice were administered according to different regimens, the changes in serum indicators of each group of mice were measured on the 1st, 3rd, 5th, 7th, 9th, and 13th day of administration. The results were shown in Figure 6. Figure 6A showed the changes of ALT content of mice in five groups on different administration days. With the prolongation of time, the serum ALT levels of the five groups of mice were gradually increased, but the increasing trend was slow, and there was no substantial difference in ALT levels among the five groups (P>0.05). Figure 6B showed the changes of AST content of mice in five groups on different days of administration. With the prolongation of time, the serum AST content of mice in groups A, B, C, and D did not show significant changes, while that of the control group showed a slight increase and then gradually recovered. No substantial difference was suggested in AST content among the five groups of mice (P>0.05).

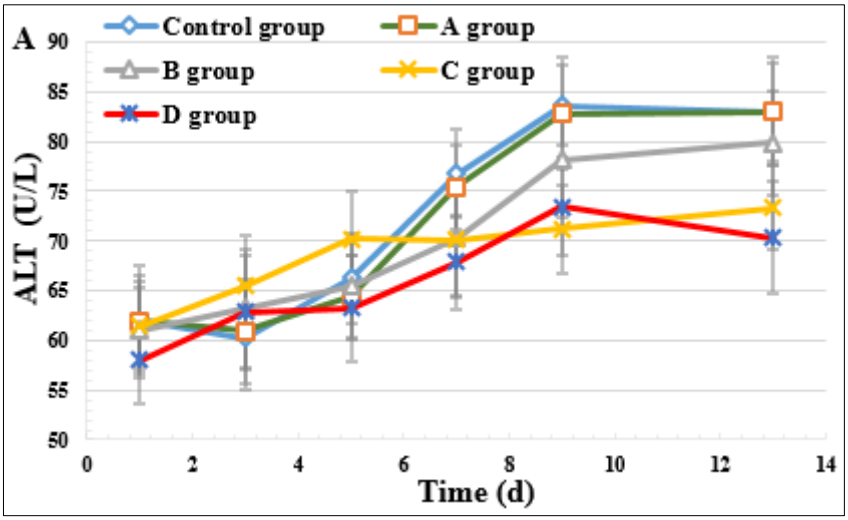

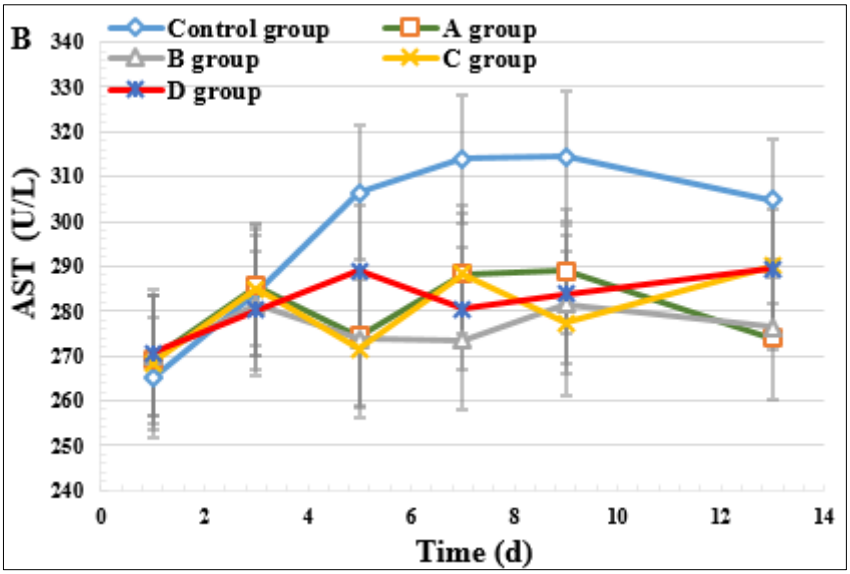

Figure 6. Changes of serum indicators in mice
Note: A: changes in ALT; B: changes in AST

3.7. Mouse tumor tissue staining results

Five groups of mice were administered, and then they were sacrificed after the administration. The tumor of the mice was round or oval, the capsule was intact, and blood vessels could be seen around the tumor. Figure 7 showed the results of HE staining of tumor tissue of mice in the five groups. The results of HE staining showed that tumor cells were diffusely distributed and were mostly round or oval. In group A and the control group, hyper-stained tumor cells were obviously arranged in crowded clusters or cords, with larger nuclei and lymphocyte infiltration around the cells. In group B, some necrotic areas were seen, and a small amount of tumor cells were distributed. In groups C and D, obvious necrotic areas or focal necrosis were seen, and lymphocyte infiltration was seen. Hence, the prepared paclitaxel-loaded SFNPs had a good inhibitory effect on the tumor growth of liver cancer model mice, that was, certain anti-tumor effect.

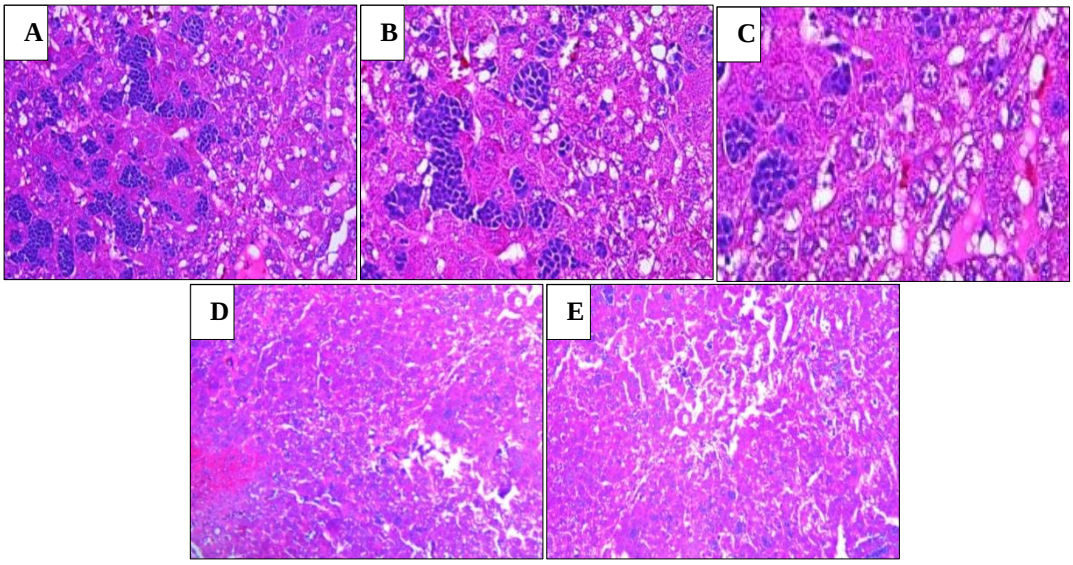

Figure 7. HE staining of mouse tumor tissue (×400)
Note: A, B, C, D, and E represented the control group, group A, group B, group C, and group D, respectively

Figure 8 showed the results of HE staining of the liver tissue of mice in the five groups. Some hepatocytes were scattered with deep nuclear staining, and some areas of hepatocytes appeared loose,

swollen, and watery. No obvious pathological changes were found in the HE staining of hepatocytes in the five groups of mice. Therefore, the prepared paclitaxel-loaded SFNPs did not cause obvious damage to the normal liver and other tissues of mice.

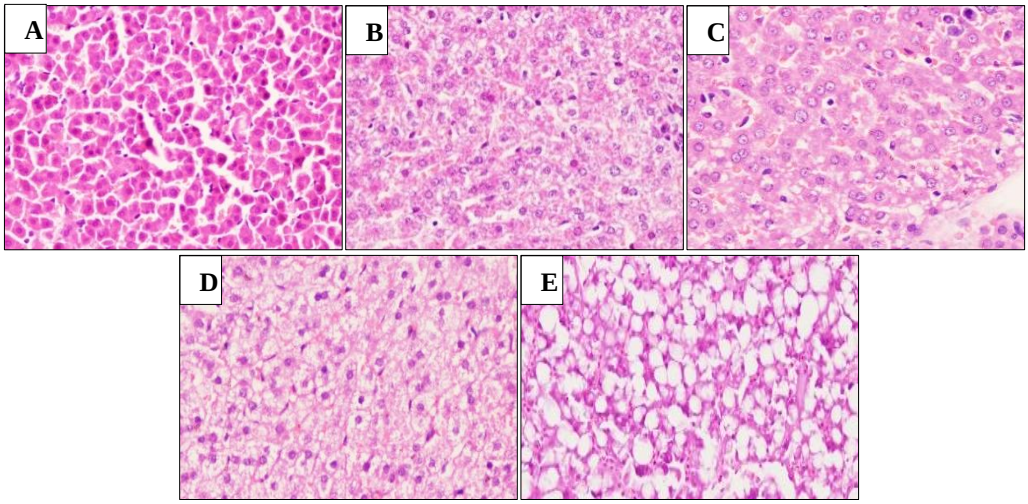

Figure 8. HE staining of mouse liver tissue (×400)
Note: A, B, C, D, and E represented the control group, group A, group B, group C, and group D, respectively

3.8. Apoptosis of tumor cells in mice

The apoptosis of tumor cells in five groups of mice was analyzed after drug intervention, and the results were shown in Figure 9. The tumor cell apoptosis rates of the mice in the five groups were 16.7, 21.33, 35.6, 46.38, and 48.23%, respectively. The tumor cell apoptosis rate in group B was greatly superior to that in the control group and group A ($P < 0.05$). Hence, paclitaxel had a certain inhibitory effect on liver cancer cells, but the inhibitory effect was weak. The apoptosis rates of tumor cells in groups C and D were greatly superior to those of the other groups ($P < 0.05$), and that of group D was greatly superior to that in group C ($P < 0.05$). It may be because the paclitaxel-loaded SFNPs enhanced the antitumor effect of the drug, and the effect of nanocarrier drug injection around the tumor was significantly better than that of intraperitoneal injection. Figure 9B showed the comparison of tumor inhibition rates of the five groups of mice. The tumor inhibition rates of five groups were 0.24, 1.28, 22.31, 54.51, and 60.23%, respectively. Among them, the tumor inhibition rates of group C and group D were greatly superior to those of the other groups ($P < 0.05$), and that of group D was greatly superior to group C ($P < 0.05$).

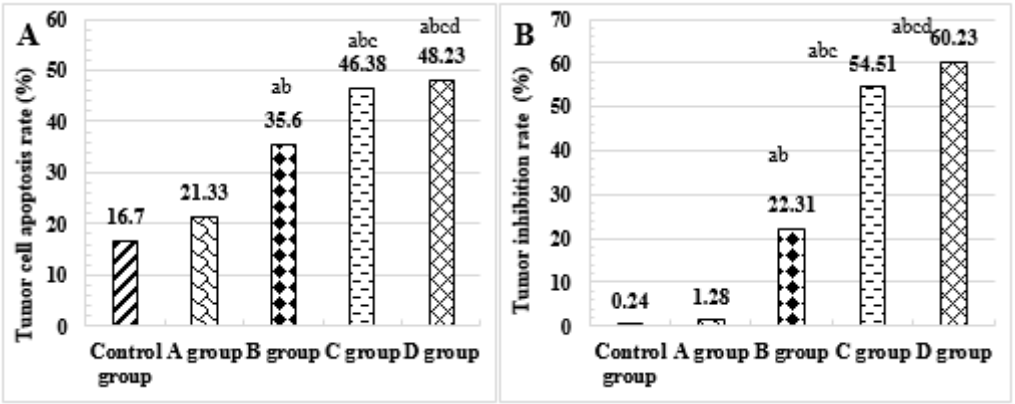

Figure 9. Apoptosis of tumor cells in mice
Note: A: tumor cell apoptosis rate; B: tumor inhibition rate
(Compared with the control group, $^{a}P < 0.05$; compared with the group A, $^{b}P < 0.05$; compared with the group B, $^{c}P < 0.05$; compared with the group C, $^{d}P < 0.05$.)

As a common malignant tumor in China, liver cancer accounts for more than 50% of liver cancer worldwide. Due to the insidious onset of hepatocellular carcinoma, patients do not show any obvious symptoms at the initial stage, so most patients have been diagnosed as intermediate and advanced stage when they are found, and the best opportunity for surgical treatment has been missed [33,34]. In addition, due to the particularity of liver cancer, no matter surgical treatment, interventional therapy, chemotherapy, or targeted drug therapy, the therapeutic effect of liver cancer is still far from ideal, and the recurrence rate is high and survival rate is low [35,36]. Currently, the drugs used to treat liver cancer are mainly through some new targeted drugs, which act on some special target molecules in the growth regulation of liver cancer [37,38]. Chemotherapy is the use of drugs to destroy cancer cells. After the drugs enter the blood and reach all areas of the body, they play a certain inhibitory or therapeutic effect on the cancer that has spread to the distal organs [39,40]. However, Li et al. (2014) [41] found that after commonly used chemotherapy drugs were introduced into patients, the amounts of drugs reaching the tumor site was far less than the total amount of drugs given because the distribution in the body could not be well controlled. In addition to killing the tumor, it is inevitable to cause certain damage to normal tissues, organs, or cells, and weaken the therapeutic effect of drugs to a certain extent [42]. With the continuous progression of science and medical level, the problem of poor distribution effect of drugs in vivo and damage to normal tissue cells of patients becomes the focus. Nanomaterials, due to their biocompatibility and small particle size, have become increasingly popular as anti-tumor drug carriers [43].

In this work, SFNPs were prepared by centrifugation, ultrasound, and other methods after being dissolved in organic solvents, and used as the carrier of the anti-tumor drug paclitaxel. To study the effect of drug-loaded nanoparticles on hepatocellular carcinoma in mice, a subcutaneous transplanted tumor model was established. H22 mouse liver cancer cell line was injected into the back of the mouse to prepare the mouse liver cancer model. One week later, when the tumor volume of the mouse reached 100 mm^3, the modeling was successful. Scanning electron microscopy showed that the prepared nanoparticles had uniform particle size, uniform distribution, no adhesion, and the average particle size was less than 500 nm. Wang et al. (2020) [44] showed that SFNPs can improve the uptake of drugs in cells, prolong the retention time of drugs, and have advantages of high efficiency, long-acting and targeting in cells, which is conducive to improving the bioavailability of drugs. The results of the changes of tumor volume in mice at different periods showed that the tumor volume of mice in group C and group D on the 7th, 9th, and 13th days of administration were dramatically smaller than those of the other groups ($P < 0.05$). And the tumor volume (154.49 ± 9.65 mm^3) of mice in group D on the 13th day of administration was dramatically smaller than that in group C (167.79 ± 9.72 mm^3) ($P < 0.05$). The tumor mass (0.89 ± 0.14 g, 0.54 ± 0.13 g, and 0.46 ± 0.11 g) of mice in groups B, C, and D was dramatically smaller than that in the other groups (1.23 ± 0.12 g and 1.24 ± 0.11 g) ($P < 0.05$), and that of group D was dramatically smaller than group B and group C ($P < 0.05$), which was similar to the results of Qian et al. (2020) [45]. It was concluded that the paclitaxel-loaded SFNPs can effectively improve the targeting effect and bioavailability of the drug, and significantly inhibit the growth of tumor cells, resulting in smaller tumor volume and lower tumor mass than other treatment groups. The apoptosis rates of tumor cells in groups C and D (46.38%, 48.23%) were greatly superior to those in the control group (16.7%), group A (21.33%), and group B (35.6%) ($P < 0.05$), and that of group D greatly superior to that in group C ($P < 0.05$). It may be because the paclitaxel-loaded SFNPs enhanced the antitumor effect of the drug, and the effect of nanocarrier drug injection around the tumor was significantly better than that of intraperitoneal injection.

5. Conclusions

SFNPs loaded with paclitaxel can effectively improve the targeting effect and bioavailability of drugs in the treatment of liver cancer, thus playing a role in improving the efficacy, which has a good application prospect. However, the in vitro cytotoxicity test was not conducted in this study, which is not representative. Therefore, the improvement and optimization in this aspect will be carried out in the

follow-up study, so as to further explore the construction of nano drug delivery system of paclitaxel and its application effect in tumor treatment. In conclusion, this work provides a theoretical basis for drug therapy and targeted therapy of tumor.

References

1.MARENGO A, ROSSO C, BUGIANESI E., Liver Cancer: Connections with Obesity, Fatty Liver, and Cirrhosis. Annu Rev Med. 2016;67:103-17.
doi: 10.1146/annurev-med-090514-013832. Epub 2015 Oct 14. PMID: 26473416.
2.SIA D, VILLANUEVA A, FRIEDMAN SL, LLOVET JM., Liver Cancer Cell of Origin, Molecular Class, and Effects on Patient Prognosis. Gastroenterology. 2017 Mar;152(4):745-761.
doi: 10.1053/j.gastro.2016.11.048. Epub 2016 Dec 30. PMID: 28043904.
3.LI L, WANG H., Heterogeneity of liver cancer and personalized therapy. Cancer Lett. 2016 Sep 1;379(2):191-7. doi: 10.1016/j.canlet.2015.07.018. Epub 2015 Jul 23. PMID: 26213370.
4.ORCUTT S.T., ANAYA D.A., Liver Resection and Surgical Strategies for Management of Primary Liver Cancer. Cancer Control. 2018 Jan-Mar;25(1):1073274817744621.
doi: 10.1177/1073274817744621. PMID: 29327594; PMCID: PMC5933574.
5.KELLY C.M., KEMENY N.E., Liver-directed therapy in metastatic colorectal cancer. Expert Rev Anticancer Ther. 2017 Aug;17(8):745-758.
doi: 10.1080/14737140.2017.1345629. Epub 2017 Jun 28. PMID: 28636427.
6.RAOUL J.L., FORNER A., BOLONDI L., CHEUNG T.T., KLOECKNER R., DE BAERE T., Updated use of TACE for hepatocellular carcinoma treatment: How and when to use it based on clinical evidence. Cancer Treat Rev. 2019 Jan;72:28-36.
doi: 10.1016/j.ctrv.2018.11.002. Epub 2018 Nov 12. PMID: 30447470.
7.ZHOU Y., LI Y., ZHOU T., ZHENG J., LI S., LI H.B., Dietary Natural Products for Prevention and Treatment of Liver Cancer. Nutrients. 2016 Mar 10;8(3):156.
doi: 10.3390/nu8030156. PMID: 26978396; PMCID: PMC4808884.
8.HAN K., KIM J.H., Transarterial chemoembolization in hepatocellular carcinoma treatment: Barcelona clinic liver cancer staging system. World J Gastroenterol. 2015 Sep 28;21(36):10327-35.
doi: 10.3748/wjg.v21.i36.10327. PMID: 26420959; PMCID: PMC4579879.
9.HEINRICH S., CRAIG A.J., MA L., HEINRICH B., GRETEN T.F., WANG X.W., Understanding tumour cell heterogeneity and its implication for immunotherapy in liver cancer using single-cell analysis. J Hepatol. 2021 Mar;74(3):700-715.
doi: 10.1016/j.jhep.2020.11.036. Epub 2020 Nov 30. PMID: 33271159.
10.CHENG Z., WEI-QI J., JIN D., New insights on sorafenib resistance in liver cancer with correlation of individualized therapy. Biochim Biophys Acta Rev Cancer. 2020 Aug;1874(1):188382.
doi: 10.1016/j.bbcan.2020.188382. Epub 2020 Jun 6. PMID: 32522600.
11.YU Y., ZHAO Y., ZHOU G., WANG X., Therapeutic Efficacy of Delta-Like Ligand 4 Gene Vaccine Overexpression on Liver Cancer in Mice. Technol Cancer Res Treat.
2020 Jan-Dec;19:1533033820942205.
doi: 10.1177/1533033820942205. PMID: 33191858; PMCID: PMC7672725.
12.LIN Z.L., DING J., SUN G.P, LI D., HE S.S., LIANG X.F., HUANG X.R., XIE J., Application of Paclitaxel-loaded EGFR Peptide-conjugated Magnetic Polymeric Liposomes for Liver Cancer Therapy. Curr Med Sci. 2020 Feb;40(1):145-154.
doi: 10.1007/s11596-020-2158-4. Epub 2020 Mar 13. PMID: 32166677.
13.CHEN L., LIU Z.X., BI Q.C., ZHAO J., LIANG Q.R., TANG Q., Ultrasound-Guided Percutaneous Ethanol-Paclitaxel Combined Therapy for Rabbit VX2 Liver Tumors. J Hepatocell Carcinoma. 2021 Apr 20;8:263-270. doi: 10.2147/JHC.S301083. PMID: 33907696; PMCID: PMC8068506.

14.LI Q., MA Z., LIU Y., KAN X., WANG C., SU B., LI Y., ZHANG Y., WANG P., LUO Y., NA D., WANG L., ZHANG G., ZHU X., WANG L., Low doses of paclitaxel enhance liver metastasis of breast cancer cells in the mouse model. FEBS J. 2016 Aug;283(15):2836-52.
doi: 10.1111/febs.13767. Epub 2016 Jun 16. PMID: 27307301.
15.INYANG K.E., MCDOUGAL T.A., RAMIREZ E.D., WILLIAMS M., LAUMET G., KAVELAARS A., HEIJNEN C.J., BURTON M., DUSSOR G., PRICE T.J., Alleviation of paclitaxel-induced mechanical hypersensitivity and hyperalgesic priming with AMPK activators in male and female mice. Neurobiol Pain. 2019 Sep 27;6:100037.
doi: 10.1016/j.ynpai.2019.100037. PMID: 31650090; PMCID: PMC6804652.
16.ZHOU L., DING L., LIU J., ZHANG Y., LUO X., ZHAO L., REN J., Four-and-a-half LIM protein 1 promotes paclitaxel resistance in hepatic carcinoma cells through the regulation of caspase-3 activation. J Cancer Res Ther. 2018 Sep;14(Supplement):S767-S773.
doi: 10.4103/0973-1482.187304. PMID: 30249901.
17.KADIFE E., CHAN E., LUWOR R., KANNOURAKIS G., FINDLAY J., AHMED N., PACLITAXEL-Induced Src Activation Is Inhibited by Dasatinib Treatment, Independently of Cancer Stem Cell Properties, in a Mouse Model of Ovarian Cancer. Cancers (Basel). 2019 Feb 19;11(2):243.
doi: 10.3390/cancers11020243. PMID: 30791462; PMCID: PMC6406511.
18.GAO Y.Y., CHEN H., ZHOU Y.Y., WANG L.T., HOU Y., XIA X.H., DING Y., Intraorgan Targeting of Gold Conjugates for Precise Liver Cancer Treatment. ACS Appl Mater Interfaces. 2017 Sep 20;9(37): 31458-31468. doi: 10.1021/acsami.7b08969. Epub 2017 Sep 5. PMID: 28838233.
19.CADAMURO M., SPAGNUOLO G., SAMBADO L., INDRACCOLO S., NARDO G., ROSATO A., BRIVIO S., CASLINI C., STECCA T., MASSANI M., BASSI N., NOVELLI E., SPIRLI C., FABRIS L., STRAZZABOSCO M., Low-Dose Paclitaxel Reduces S100A4 Nuclear Import to Inhibit Invasion and Hematogenous Metastasis of Cholangio-carcinoma. Cancer Res. 2016 Aug 15;76(16): 4775-84.
doi: 10.1158/0008-5472.CAN-16-0188. Epub 2016 Jun 21. PMID: 27328733; PMCID: PMC4987167.
20.LI S.S., ZHANG C.M., WU J.D., LIU C., LIU Z.P., A branched small molecule-drug conjugate nanomedicine strategy for the targeted HCC chemotherapy. Eur J Med Chem. 2022 Jan 15;228:114037.
doi: 10.1016/j.ejmech.2021.114037. Epub 2021 Dec 2. PMID: 34883290.
21.PAN Z.Q., FANG Z.Q., LU W.L., [Characteristics of gene expression of adrenal cortical steroid synthetase and its regulatory factor in mice with H22 liver cancer of different patterns]. Zhongguo Zhong Xi Yi Jie He Za Zhi. 2011 Jan;31(1):85-9. Chinese. PMID: 21434351.
22.WANG P.P., WANG Y.H., WANG L.S., WU T., [Anti-tumor effect and its related mechanisms of cinobufotalin combined with cisplatin on H22 liver cancer mice]. Zhongguo Zhong Yao Za Zhi. 2020 Aug;45(16):3945-3951. Chinese. doi: 10.19540/j.cnki.cjcmm.20200224.401. PMID: 32893593.
23.ZHU Q, CHEN J, LI Q, WANG T, LI H. Antitumor activity of polysaccharide from Laminaria japonica on mice bearing H22 liver cancer. Int J Biol Macromol. 2016 Nov;92:156-158.
doi: 10.1016/j.ijbiomac.2016.06.090. Epub 2016 Jun 29. PMID: 27375056.
24.CHENG W., MIAO L., ZHANG H., YANG O., GE H., LI Y., WANG L., Induction of interleukin 2 expression in the liver for the treatment of H22 hepatoma in mice. Dig Liver Dis. 2013 Jan;45(1):50-7.
doi: 10.1016/j.dld.2012.08.014. Epub 2012 Sep 19. PMID: 22999060.
25.DING Z., WANG D., SHI W., YANG X., DUAN S., MO F., HOU X., LIU A., LU X., In vivo Targeting of Liver Cancer with Tissue- and Nuclei-Specific Mesoporous Silica Nanoparticle-Based Nanocarriers in mice. Int J Nanomedicine. 2020 Oct 29;15:8383-8400.
doi: 10.2147/IJN.S272495. PMID: 33149582; PMCID: PMC7605659.
26.LI S., ZHENG L., Effect of Combined Treatment Using Wilfortrine and Paclitaxel in Liver Cancer and Related Mechanism. Med Sci Monit. 2016 Apr 4;22:1109-14.
doi: 10.12659/msm.896197. PMID: 27043783; PMCID: PMC4822940.

27.ZHOU F., TENG F., DENG P., MENG N., SONG Z., FENG R., Recent Progress of Nano-drug Delivery System for Liver Cancer Treatment. Anticancer Agents Med Chem. 2018 Feb 7;17(14):1884-1897. doi: 10.2174/1871520617666170713151149. PMID: 28707574.
28.HONG H., SEO Y.B., KIM D.Y., LEE J.S., LEE Y.J., LEE H., AJITERU O., SULTAN MT., LEE OJ., KIM S.H., PARK C.H., Digital light processing 3D printed silk fibroin hydrogel for cartilage tissue engineering. Biomaterials. 2020 Feb;232:119679.
doi: 10.1016/j.biomaterials.2019.119679. Epub 2019 Dec 13. PMID: 31865191.
29.LIU J., HUANG R., LI G., KAPLAN D.L., ZHENG Z., WANG X., Generation of Nano-pores in Silk Fibroin Films Using Silk Nanoparticles for Full-Thickness Wound Healing. Biomacromolecules. 2021 Feb 8;22(2):546-556. doi: 10.1021/acs.biomac.0c01411. Epub 2021 Jan 15. PMID: 33449619.
30.HUDITA A., RADU I.C., GALATEANU B., GINGHINA O., HERMAN H., BALTA C., ROSU M., ZAHARIA C., COSTACHE M., TANASA E., VELONIA K., TSATSAKIS A., HERMENEAN A., Bioinspired silk fibroin nano-delivery systems protect against 5-FU induced gastrointestinal mucositis in a mouse model and display antitumor effects on HT-29 colorectal cancer cells *in vitro*. Nanotoxicology. 2021 Sep;15(7):973-994.
doi: 10.1080/17435390.2021.1943032. Epub 2021 Jul 2. PMID: 34213984.
31.REZAEI F., KESHVARI H., SHOKRGOZAR MA., DOROUD D., GHOLAMI E., KHABIRI A., FAROKHI M., Nano-adjuvant based on silk fibroin for the delivery of recombinant hepatitis B surface antigen. Biomater Sci. 2021 Apr 7;9(7):2679-2695.
doi: 10.1039/d0bm01518k. Epub 2021 Feb 19. PMID: 33605970.
32.KIM J., LEE S., NA K., Glycyrrhetinic Acid-Modified Silicon Phthalocyanine for Liver Cancer-Targeted Photodynamic Therapy. Biomacromolecules. 2021 Feb 8;22(2):811-822.
doi: 10.1021/acs.biomac.0c01550. Epub 2020 Dec 28. PMID: 33356155.
33.GAO Y., HU L., LIU Y., XU X., WU C., Targeted Delivery of Paclitaxel in Liver Cancer Using Hyaluronic Acid Functionalized Mesoporous Hollow Alumina Nanoparticles. Biomed Res Int. 2019 Apr 15;2019:2928507. doi: 10.1155/2019/2928507. PMID: 31119162; PMCID: PMC6500713.
34.WANG L., NAN X., HOU J., XIA Y., GUO Y., MENG K., XU C., LIAN J., ZHANG Y., WANG X., ZHAO B., Preparation and biological properties of silk fibroin/nano-hydroxyapatite/hyaluronic acid composite scaffold. Biomed Mater. 2021 Jun 25;16(4).
doi: 10.1088/1748-605X/ac08aa. PMID: 34098538.
35.DONG S., ZHANG Y., LI B., REN J., LING S., CAO L., Self-adhesive and contractile silk fibroin/graphene nano-ionotronic skin for strain sensing of irregular surfaces. Nanotechnology. 2021 Sep 1;32(47). doi: 10.1088/1361-6528/ac137e. PMID: 34252892.
36.LI L., CHEN D., ZHENG K., JIANG L., DAI T., YANG L., JIANG L., CHEN Z., YUAN C., HUANG M., Enhanced Antitumor Efficacy and Imaging Application of Photosensitizer-Formulated Paclitaxel. ACS Appl Mater Interfaces. 2020 Jan 29;12(4):4221-4230.
doi: 10.1021/acsami.9b18396. Epub 2020 Jan 17. PMID: 31909969.
37.ZHAO L., LIANG L., GUO M., LI M., YU X., WANG Y., WANG Y., Hepatocellular Carcinoma Targeting and Pharmacodynamics of Paclitaxel Nanoliposomes Modified by Glycyrrhetinic Acid and Ferric Tetroxide. Curr Top Med Chem. 2021 Oct 5;21(14):1268-1284.
doi: 10.2174/1568026621666210621090005. PMID: 34620053.
38.Al-SHAKARCHI W., ALSURAIFI A., CURTIS A., HOSKINS C., Dual Acting Polymeric Nano-Aggregates for Liver Cancer Therapy. Pharmaceutics. 2018 May 26;10(2):63.
doi: 10.3390/pharmaceutics10020063. PMID: 29861445; PMCID: PMC6027472.
39.SHEN W., GE S., LIU X., YU Q., JIANG X., WU Q., TIAN Y., GAO Y., LIU Y., WU C., Folate-functionalized SMMC-7721 liver cancer cell membrane-cloaked paclitaxel nanocrystals for targeted chemotherapy of hepatoma. Drug Deliv. 2022 Dec;29(1):31-42.
doi: 10.1080/10717544.2021.2015481. PMID: 34962215; PMCID: PMC8725828.

40.WANG H., ELLIPILLI S., LEE W.J., LI X., VIEWEGER M., HO Y.S., GUO P., Multivalent rubber-like RNA nanoparticles for targeted co-delivery of paclitaxel and MiRNA to silence the drug efflux transporter and liver cancer drug resistance. J Control Release. 2021 Feb 10;330:173-184. doi: 10.1016/j.jconrel.2020.12.007. Epub 2020 Dec 13. PMID: 33316298; PMCID: PMC7923242.
41.LI Y.R., WANG J.R., ZHANG H.Y., WU X.F., LI S.N., WANG L., WANG X.Y., Dynamic morphological examination and evaluation of biological characteristics of a multinodular liver cancer model in mice. Lab Anim. 2014 Apr;48(2):132-42. doi: 10.1177/0023677213516310. Epub 2013 Dec 20. PMID: 24362593.
42.FU XD, ZHANG YY, WANG XJ, SHOU JX, ZHANG ZZ, SONG LJ. Preparation and biological activity of a paclitaxel-single-walled carbon nanotube complex. Genet Mol Res. 2014 Mar 12;13(1): 1589-603. doi: 10.4238/2014.March.12.11. PMID: 24668633.
43.WU C., GAO Y., LIU Y., XU X., Pure paclitaxel nanoparticles: preparation, characterization, and antitumor effect for human liver cancer SMMC-7721 cells. Int J Nanomedicine. 2018 Oct 9;13:6189-6198. doi: 10.2147/IJN.S169209. PMID: 30349243; PMCID: PMC6188176.
44.WANG X., LI M., WANG J., CAO Y., The Effect of Nano-Albumin Paclitaxel on the Early Postoperative Recurrence of Primary Liver Cancer. J Nanosci Nanotechnol. 2020 Dec 1;20(12):7283-7288. doi: 10.1166/jnn.2020.18710. PMID: 32711592.
45.QIAN K.Y., SONG Y., YAN X., DONG L., XUE J., XU Y., WANG B., CAO B., HOU Q., PENG W., HU J., JIANG K., CHEN S., WANG H., LU Y., Injectable ferrimagnetic silk fibroin hydrogel for magnetic hyperthermia ablation of deep tumor. Biomaterials. 2020 Nov; 259:120299. doi: 10.1016/j.biomaterials.2020.120299. Epub 2020 Aug 10. PMID: 32827797

Manuscript received: 6.03.2022